Forcing-type-dependent stability of steady states in a turbulent swirling flow

B. Saint-Michel,[1,*] B. Dubrulle,[1] L. Marié,[2] F. Ravelet,[3] and F. Daviaud[1]

[1] *Laboratoire SPHYNX, Service de Physique de l'État Condensé, DSM, CEA Saclay, CNRS URA 2464, 91191 Gif-sur-Yvette, France*
[2] *Laboratoire de Physique des Océans, UMR 6523 CNRS/IFREMER/IRD/UBO, Brest, France*
[3] *Laboratoire Dynfluid, ENSAM ParisTech, CNRS EA92, 151, boulevard de l'Hôpital 75013 Paris, France*

We study the influence of the forcing on the steady turbulent states of a von Kármán swirling flow, at constant impeller speed, or at constant torque. We find that the different forcing conditions change the nature of the stability of the steady states and reveal dynamical regimes that bear similarities with low-dimensional systems. We suggest that this forcing dependence may be an analogue of the *ensemble inequivalence* observed in long-range interacting statistical systems, and that it may be applicable to other turbulent systems.

PACS numbers: 47.20.Ky, 05.45.-a, 47.27.Sd

Introduction An intriguing property of statistical systems with long range interactions is the *ensemble inequivalence*: a solution in the microcanonical (constrained) ensemble is not necessarily a solution in the canonical (unconstrained) ensemble [1, 2]. This property traces back to the non-additivity of energy, and is reflected by pathological behaviours of the entropy (that can be non-concave) or the heat capacity (that can become negative). Ensemble inequivalence has been observed and studied in a variety of systems such as 2D Euler equations [3, 4], Blume-Emery-Griffiths model [5], and random graphs [6]. More recently, it has been studied in a model describing the one-dimensional motion of rotators coupled through mean-field interaction, and subjected to the perturbation of an external magnetic field [7]; it shows that this concept may also hold out of equilibrium, broadening its range of applicability. Nevertheless, a generalisation of such concepts to all out-of-equilibrium systems remains an open question. We propose an extension of such tools to turbulent systems. They naturally display long-range interactions and are, by definition, far from equilibrium. Our system is a "von Kármán" experiment, a cylinder of fluid stirred by two counter-rotating impellers, producing fully-developed turbulence in a small experimental device. Several features of equilibrium systems have already been described in this model experiment, such as steady states, predicted by the resolution of the axisymmetric Euler equations [8], hysteresis [9], and spontaneous symmetry-breaking with diverging susceptibility [10].

In this letter, we will examine the stability of such statistically steady states under two different forcing conditions, either imposing the *speed* or the *torque* — flux of kinetic momentum [11] — to our impellers. The subject has attracted little attention, work focusing on the difference of power fluctuations [12–14] under both conditions. However, we can consider our forcings to be conjugate, the product torque × speed controlling the energy injection rate. Switching from speed to torque control might then be seen as an analogue of switching from *canonical* to *microcanonical* ensemble; it is shown to alter the stability of the steady states previously observed in [9] and to reveal interesting dynamical regimes.

Experimental setup The von Kármán flow is created in a polycarbonate cylinder of inner radius $R = 100$ mm filled with water. The fluid is stirred by two impellers of radius $0.925R$ fitted with 8 curved blades. The impellers are separated from each other by a distance $1.4R$. Two independent 1.8 kW brush-less motors can rotate the impellers either by imposing their speeds (f_1, f_2) or their torques (C_1, C_2). Torque and speed measurements are performed by two Scaime MR12 torque sensors fixed to the mechanical shafts driving the impellers. Fluid confinement is assured by two balanced mechanical seals under a 2.8 bar pressure to provide minimum friction. Temperature is regulated by an external water flow in two refrigeration coils installed behind each impeller. The Reynolds number of our experiment, defined as $Re = \pi(f_1+f_2)R^2/\nu$, and varying from $2{\cdot}10^5$ to $5{\cdot}10^5$, is well above the transition to turbulence reported in [15].

Our experiments aim to measure the response of the flow to asymmetric forcing for both types of controls. *Speed* control experiments will impose $(f_1 + f_2)/2 = 4$ Hz, to study the influence of $f_1 \neq f_2$ on the values of C_1 and C_2. Reciprocally, *torque* control fixes $(C_1+C_2)/2 = 1.72$ Nm to study the effect of torque asymmetries on the impeller speeds f_1 and f_2. The upside-down $\mathcal{R}_\pi$ symmetry (see inset in fig 1) provides a definition of two antisymmetric dimensionless quantities θ and γ to measure the forcing — and response — asymmetry: $\theta = (f_1 - f_2)/(f_1 + f_2)$ is the reduced impeller *speed* difference and $\gamma = (C_1 - C_2)/(C_1 + C_2)$ is the reduced shaft *torque* difference.

Speed control For speed-imposed experiments, all turbulent flows are statistically steady. These steady states are characterized by their mean torque asymmetry γ. Starting both impellers at the same time for θ very close to 0, the system reaches steady states corresponding to a 'symmetric' branch called (s). The average flow in this regime consists of two Ekman recirculation cells sepa-

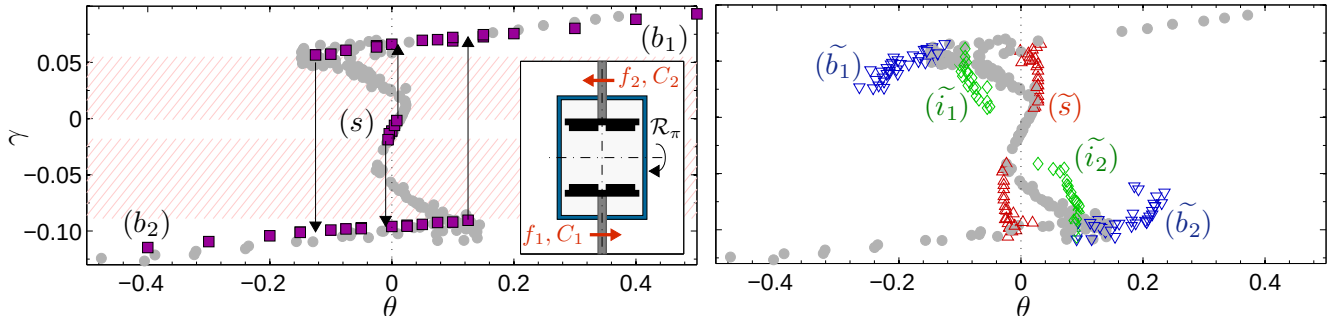

FIG. 1: (Left), mean reduced torque asymmetry γ plotted as a function of the mean reduced speed asymmetry θ, for both speed (purple squares) and torque (grey circles) experiments. The arrows indicate the possible transitions between steady states, sketching a hysteresis cycle including a forbidden γ zone (hatched region) for *speed control* experiments. No hysteresis is observed in *torque control*. (Right), modes of the θ p.d.f for torque control experiments corresponding to the 'forbidden range'. $(\tilde{s})$, $(\tilde{b_1})$ and $(\tilde{b_2})$ are quasi-steady states branches extending respectively the steady (s), (b_1) and (b_2) branches. $(\tilde{i_1})$ and $(\tilde{i_2})$ are new branches, never observed in speed control. (Inset) Sketch of the 'VK2' experiment, with the two impellers (black). The experiment is axisymmetric along the vertical axis, and is $\mathcal{R}_\pi$ symmetric for exact counter-rotation.

rated by a shear layer, in agreement with [9, 10]. In such states, a small θ variation triggers a transition with a dramatic increase of the mean torque. These new 'bifurcated' states exhibit — in average — only one circulation cell, and form two separate branches of the (γ, θ) plane (see fig. 1, left). These branches, named (b_1) and (b_2), respectively exhibit a global pumping of the bottom or the top impeller. Velocimetry measurements have confirmed that the velocity fields of the flows belonging to the (b_1) and (b_2) are images of each other by the $\mathcal{R}_\pi$ rotation, restoring globally the experimental symmetries. Once on (b_1) and (b_2) branches, the (s) state cannot be reached, which is therefore marginally stable. In addition, the (b_1) and (b_2) branches are hysteretic, (b_1) states persisting for $f_1 \leq f_2$ and (b_2) states for $f_2 \leq f_1$ [16], agreeing with previous results [9]. This hysteresis is associated with a 'forbidden zone' of γ values never accessed for imposed speed.

Torque control In contrast, imposing *torque* allows *any* value of γ assuming friction is negligible. We have first verified that imposing γ out of the 'forbidden zone' provides steady states identical to those observed in speed control, following the branches already described in fig. 1. Such flows are almost identical to speed-control flows, no difference in velocimetry measurements being visible after suitable normalization. Our experiments have then focused on the henceforth accessible 'forbidden zone'. In this region, the system looses steadiness: the impeller speed may alternatively jump between multiple attracting turbulent states. This multi-stability is identified by the emergence of multiple local maxima in the p.d.f. (probability density function) of the 1.5 Hz low-pass filtered signal of $\theta(t)$. Such filtering is required considering the discrete nature of our speed measurements; it yields a robust density function when the filter cutoff frequency is changed. Three types of attracting states have then been identified: $(\tilde{s})$, the high-speed state, is similar to (s); $(\tilde{b_1})$ and $(\tilde{b_2})$ are low-speed states similar to (b_1) and (b_2); and two new $(\tilde{i_1})$ and $(\tilde{i_2})$ *intermediate* states. These new states can be seen in fig. 1: while $(\tilde{s})$, $(\tilde{b_1})$ and $(\tilde{b_2})$ states extend their speed-imposed counterparts, $(\tilde{i_1})$ and $(\tilde{i_2})$ branches are new and cannot be observed in speed control. Decreasing γ from a perfectly symmetric $(\tilde{s})$ $(\theta = 0)$ state, we can observe the asymmetry influence on temporal signals of the impeller speeds, as done in fig. 2. First, steady states with decreasing mean θ are observed. Then (fig. 2*b*), when $\gamma \leq -0.049$ — a local extremum of the mean value of θ — small localized peaks of f_1 and f_2 are simultaneously observed, breaking time invariance. Such events are identified as excursions towards intermediate state $(\tilde{i_2})$. Still decreasing γ, the peaks grow until the biggest events saturate at low f_1 and f_2 (fig. 2*c*). These events are identified as transitions to the $(\tilde{b_2})$ state. For even lower values of γ, the system behavior is irregular, switching between fast $(\tilde{s})$, $(\tilde{i_2})$ and slow $(\tilde{b_2})$ states (fig. 2*d*). In this situation, all states are found to be quasi-steady, each being able to last more than 10 sec. (70 impeller rotations). Decreasing further γ affects the dynamics of the system, more time being spent in $(\tilde{b_2})$ at the expense of $(\tilde{i_2})$ and $(\tilde{s})$. Therefore, for low $\gamma \geq -0.0920$ (fig. 2*e*), only rare events can drive the system to the faster $(\tilde{i_2})$ and $(\tilde{s})$ states. Eventually, for $\gamma \leq -0.099$ (fig. 2*f*), the system time-invariance is restored, corresponding to a (b_2) steady state of fig. 1. Remarkably, the flow susceptibility defined using θ mean value, $\partial\gamma/\partial\theta$, is *negative* in all this forbidden zone (see fig. 1). Obviously, *increasing* γ from a perfectly symmetric state leads to the same sequence of events, though $(\tilde{i_1})$ and $(\tilde{b_1})$ will be reached.

Valuable information about our system dynamics can be found studying near-transition variations of global quantities [17]. We have therefore superposed in fig. 3 the speed signals close to the transitions observed in fig. 2*c*: $(\tilde{s}) \rightarrow (\tilde{b_{1,2}})$ is called a down transition, and $(\tilde{b_{1,2}}) \rightarrow$

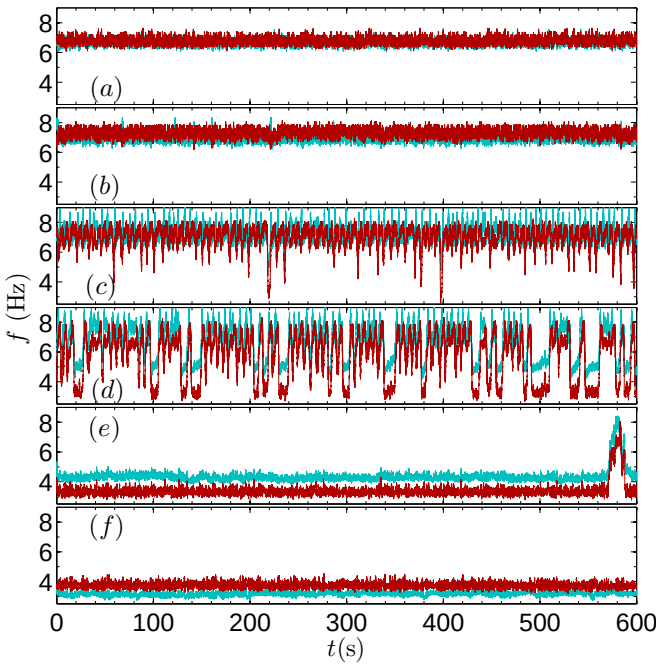

FIG. 2: Temporal series of the impeller speeds f_1 (blue) and f_2 (red) for various γ. (a), steady high-speed state $(\tilde{s})$ observed at $\gamma = -0.0164$; (b), threshold of the irregular peaks $(\tilde{i_2})$ with very small events for $\gamma = -0.0460$; (c), $(\tilde{i_2})$ irregular peaks for $\gamma = -0.0668$; (d), multi-stable regime showing $(\tilde{s})$, $(\tilde{i_2})$ and $(\tilde{b_2})$ events at $\gamma = -0.0891$; (e), single fast rare event in an almost steady slow $(\tilde{b_2})$ regime for $\gamma = -0.0912$; (f), steady slow (b_2) regime for $\gamma = -0.1049$.

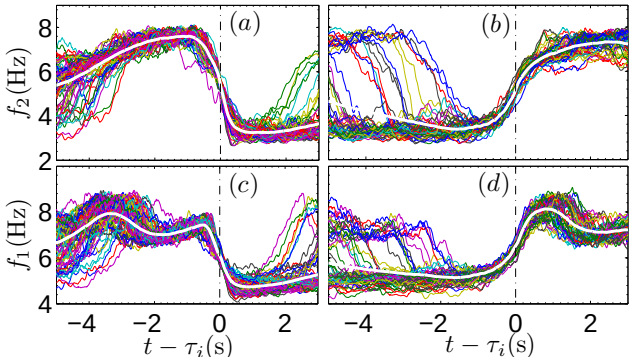

FIG. 3: Shifted temporal signals of 60 randomly-chosen transitions of a 2-hours experiment with $\gamma = -0.0891$ (same experiment as fig. 2d). We compute τ_i by finding the minimum of $|\partial_t \tilde{f_2}|$, the 1 Hz filtered signal of f_2. (a), (c), respectively f_2 and f_1 profiles for down transitions. (b), (d), respectively f_2 and f_1 for up transitions. The thick white line represents in each sub-plot the rotation frequency averaged on all 195 events of the experiment.

$(\tilde{s})$ an up transition. For every transition, we compute the transition instants τ_i as the inflection point of the — 1 Hz filtered — speed of the most forced impeller (in fig. 3, f_2): this value is then used for the two impellers. Once the value of τ_i accurately computed, a good collapse of all trans itions is observed, validating a single path for all up transitions, and another single one for down transitions. This extends the low-dimensional system description of [17] to purely hydrodynamical quantities in a non-magnetic turbulent flow. Eventually, the joint distributions of (f_1, f_2) are studied to highlight the attractors emerging from figs. 1 and 2. In fig. 4a, for small γ, only one maximum appears, which confirms the steady nature of the system in (s). For higher asymmetries, small excursions escaping the attractor — the previously described small $(\tilde{i_2})$ peaks — can be found, exhibiting a new local maximum strongly deviating from the diagonal $f_1 = f_2$. Still increasing the asymmetry, the system fills a large part of the (f_1, f_2) plane, with three main maxima: $(\tilde{s})$ close to the diagonal at higher (f_1, f_2), and $(\tilde{b_2})$ off-diagonal for low (f_1, f_2). The third — (i_2) — attractor is harder to see, being hidden by neighboring zones repeatedly crossed by unsteady events. It is located between near the right tip of the histogram. With this representation, one observes a different mean path for down and up transitions: while the down transition starts "looping" next to $(\tilde{s})$ before abruptly transiting to $(\tilde{b_2})$, the up transition reaches the right tip of the joint-pdf $(f_1 > f_2)$, near $(\tilde{i_2})$ before joining the $(\tilde{s})$ state.

The maxima height repartition of fig. 4c, (d), (e) is obviously driven by γ, from almost-fully $(\tilde{s})$, $(\tilde{i_2})$ to nearly-pure $(\tilde{b_2})$ with rare, large transitions to the faster states. For nearly-pure $(\tilde{s})$, we clearly see (fig .4c) a large amount of small excursions, contrasting with the nearly-pure $(\tilde{b_2})$ state (fig .4e), for which a small number of large events is reported. The location of such maxima depends on γ: fig. 1 recalls the γ variation of such positions. Interestingly, while the $(\tilde{b})$ and $(\tilde{s})$ abscissae increase with γ, the $(\tilde{i})$ abscissa *decreases* with γ.

Discussion Using global torque and speed measurements, we have characterized the response of the von Kármán experiment to different energy injection mechanisms. The two responses coincide in the range of parameters accessible to speed control, reproducing the hysteresis cycle previously reported by [9]. However, imposing the torque γ in the zone inaccessible in speed control generate new continuous "mean" branches connecting symmetric (s) and bifurcated (b) branches. The mean values of the speed asymmetry θ hide the underlying phenomena observed in this forbidden zone, revealing multiple local maxima of the p.d.f. of θ, each corresponding to a quasi-steady state. Two of them can be defined by continuity of the steady, speed-control branches: $(\tilde{s})$ and $(\tilde{b})$. The third state, $(\tilde{i})$, is never observed in any speed-imposed experiment. The study of the impellers velocity $f_1(t), f_2(t)$ signals shows typical excursions and transitions between our three states, similarly to [18, 19], while preliminary results on the distribution of $(\tilde{b})$ residence time favor exponential Kramers-like escape times (see fig. 5) where the longer characteristic time increases when

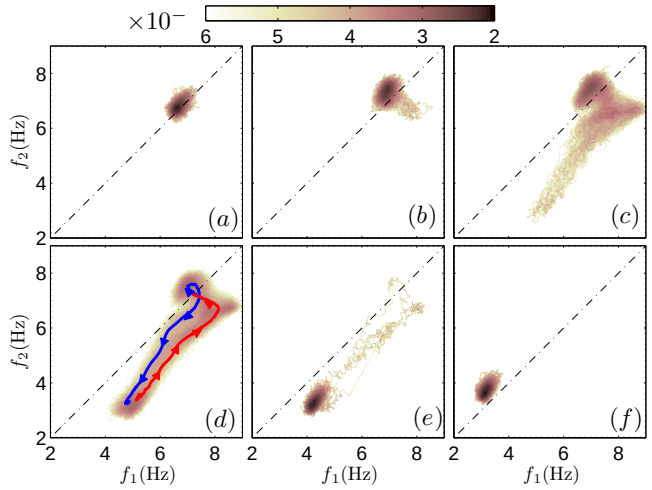

FIG. 4: Joint-probability density maps of the (f_1, f_2) values (log-scale), for the same experiments (and γ values) as fig. 2: (a), steady symmetric high-speed state; (b), beginning of irregular peaks towards an intermediate state; (c), typical irregular peaks with large slowdowns; (d), multi-stability with three 'most visited' states, (—) and (—) represent respectively the fig. 3 mean profile for down and up transitions; (e), rare events; (f), steady slow state. The black dashed-dotted line represents the $\theta = 0$ condition. Both fast and slow states can be observed at $\theta = 0$ considering the shape of fig. 1.

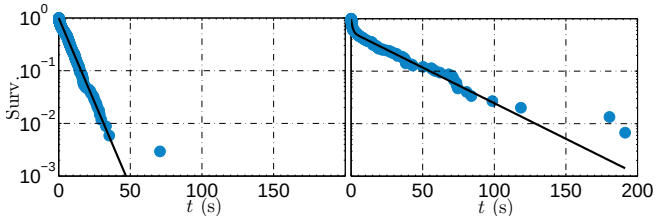

FIG. 5: Survival function $1-\int p.d.f.$ of the distribution of the time spent in the slow quasi-steady state $(\tilde{b_1})$ before up transitions. Blue (•), experimental data; solid line, exponential fit with two characteristic times. Left, $\gamma = -0.094$ favors a simple exponential distribution. Right, $\gamma = -0.097$, closer to the edge of the steady (b_2) branch, favors separate characteristic times.

approaching the bifurcated (b_2) steady branch. This confirms a "potential well" interpretation of the quasi-steady states as previously performed by [20].

Our results address several questions. The most striking result is the multi-valued asymmetry response curve, $\gamma(\theta)$. Interestingly, solid state devices can *also* display similar multivalued characteristic curves $i(U)$ [21]. It is therefore tempting to draw an electrical analogy between the von Kármán flow and an electrical dipole, where the flux of angular momentum through the flow, fixed by setting the motor torques, would be analogous to the flow of electric charges through the dipole, the role of the applied voltage U being played by the impeller speeds. In that respect, our system bears similarities with "bulk" negative differential resistances [22]. However, in all cases, negative resistances are associated with a spatial phase separation which cannot be sustained by our hydrodynamical, strongly correlated experiment.

More generally, from a statistical physics point of view, the von Kármán experiment allows a quantitative analysis of the energy injection mechanism influence on the response of an out-of-equilibrium system. In that respect, negative responses are characteristic of long-range i nteracting (LRI) systems, where ensemble inequivalence has been studied [23]. For such systems, switching from micro-canonical ensemble, with fixed energy density e, to canonical ensemble where the temperature T is imposed, can result in different sets of equilibrium states. Micro-canonical solutions can interestingly display stable regions with a negative specific heat $c_v = \partial e/\partial T$ — another analogue of negative susceptibility $\partial\gamma/\partial\theta$ and negative conductivity $\partial i/\partial U$ — . In contrast, canonical solutions always impose $c_v \geq 0$ to avoid thermal reservoir instability [5]. Imposing the impeller speed (or the applied voltage) can therefore be seen as a canonical exploration of the system response, whereas imposing the torque (or the current) is an equivalent of micro-canonical ensemble exploration, allowing negative average susceptibilities (or resistances). Eventually, the dynamic multi-stability observed in the forbidden zone can be seen as a probing of metastable quasi-steady states due to out-of-equilibrium turbulent noise, or as temporal heterogeneities in a strongly correlated system for which no "spatial phase separation" is accepted.

From the point of view of turbulence, the multivalued region sets the problem of *universality* of the steady states, that appears to be rather sensitive — on large scales — to the energy injection mechanisms, at variance with traditional view of turbulence. The phenomenon we explore in the present letter could be present in other turbulent experimental systems: (i) in turbulent Plane-Couette flows forced either with constant global stress (motor torque C) or strain (speed f); (ii) in Poiseuille flows either imposing a pressure difference, corresponding to our speed control, or a mass flow-rate, equivalent of our imposed torque [24]; (iii) in Rayleigh-Bénard convection using either temperature imposed (equivalent of a constant speed) or heat-flux imposed (analogue to torque control) boundary conditions. In particular, it would be interesting to investigate the stability of the multiple steady states observed in thermal convection at very high Rayleigh numbers [25].

Acknowledgements We thank the CNRS and CEA for support, Vincent Padilla for building the experimental device, Guillaume Mancel for sharing experimental data, and Cécile Wiertel-Gasquet for writing the acquisition programs.

* Electronic address: brice.saint-michel@cea.fr

[1] W. Thirring, Z. Phys. A, **235**, 339-352 (1970)
[2] R.S. Ellis, K. Haven and B. Turkington, J. Stat. Phys. **101**, 999 (2000)
[3] C. Herbert, B. Dubrulle, P.-H. Chavanis and D. Paillard, Phys. Rev. E, **85**, 5, 056304 (2012)
[4] A. Venaille and F. Bouchet, Phys. Rev. Lett., **102**, 10, 104501 (2009)
[5] J. Barré, D. Mukamel, S. Ruffo, Phys. Rev. Lett., **87**, 3, 030601 (2001); M.J. Blume, V.J. Emery, R.B. Griffiths, Phys. Rev. A, **4**, 1071-1077 (1971)
[6] J. Barré and B. Goncalves, Physica A 386, 212-218 (2007).
[7] G. De Ninno and D. Fanelli, Europhys. Lett., 97 20002 (2012).
[8] R. Monchaux, F. Ravelet, B. Dubrulle, A. Chiffaudel and F. Daviaud, Phys. Rev. Lett., **96**, 12, 124502 (2006)
[9] F. Ravelet, L. Marié, A. Chiffaudel and F. Daviaud, Phys. Rev. Lett., **93**, 16, 164501 (2004)
[10] P.-P. Cortet, E. Herbert, A. Chiffaudel, F. Daviaud, B. Dubrulle and V. Padilla, J. Stat. Mech. Theor. Exp., **2011**, 07, P07012 (2011); P.-P. Cortet, A. Chiffaudel, F. Daviaud and B. Dubrulle, Phys. Rev. Lett., **105**, 214501 (2010)
[11] L. Marié and F. Daviaud, Phys. Fluids, **16**, 457 (2004)
[12] J.H. Titon and O. Cadot, Phys. Fluids, **15**, 625 (2003)
[13] N. Leprovost, L. Marié and B. Dubrulle, European Physical Journal B 39 (2004) 121-129
[14] S. T. Bramwell, P. C. W. Holdsworth and J.-F. Pinton, Nature, **396**, 552-554 (1998)
[15] F. Ravelet, A. Chiffaudel and F. Daviaud, J. Fluid Mech., **601**, 339-364 (2008)
[16] This range, as well as fig. 1 do not exactly respect $\mathcal{R}_\pi$ symmetry. It is actually very difficult to obtain accurate symmetric calibrations because such experiments require small and accurate torques.
[17] M. Berhanu *et al.*, Europhys. Lett., **77**, 5 (2007)
[18] F. Pétrélis and S. Fauve, J. Phys.: Condens. Matter, **20**, 494203 (2008)
[19] F. Pétrélis, S. Fauve, E. Dormy and J.-P. Valet, Phys. Rev. Lett., **102**, 144503 (2009)
[20] A. de la Torre and J. Burguete, Phys. Rev. Lett, **99**, 054101 (2007)
[21] L. Esaki, Phys. Rev., **109**, 603–604 (1958)
[22] B.K. Ridley, Proc. Phys. Soc., **82**, 954 (1963)
[23] T. Dauxois, S. Ruffo, E. Arimondo and M. Wilkens, *Dynamics and thermodynamics of systems with long range interactions*, (Springer, 2003)
[24] A. G. Darbyshire and T. Mullin, J. Fluid Mech, **289**, 3, 83-114 (1995)
[25] G. Ahlers, D. Funfschilling and E. Bodenschatz, *New J. Phys.*, **11**, 049401 (2009)